


 Cite this: *RSC Adv.*, 2026, **16**, 11594

# Novel method for producing plasticised PLA films: method, materials, and characterization

 Gerardo Coppola,<sup>a</sup> Sebastiano Candamano,<sup>b</sup> Catia Algieri,<sup>id</sup> <sup>c</sup> Corradino Sposato,<sup>d</sup> Chiara Morano,<sup>b</sup> Leonardo Pagnotta,<sup>b</sup> Mariano Davoli,<sup>e</sup> Stefano Curcio<sup>\*a</sup> and Sudip Chakraborty<sup>id</sup> <sup>\*afg</sup>

A novel casting method for producing plasticised PLA films, intended for food packaging and biomedical applications, is presented in this current work. This method involves air-induced, temperature-controlled phase separation (AITCPS), which enables the formation of highly dense PLA matrices. A broad study is provided to understand the effects of glycerol used as a plasticizer on various physiochemical properties including morphological, thermal, mechanical, and interfacial properties, as well as water vapor transmission rates and antimicrobial activities. The results demonstrate how the plasticizer ratio has a minimal impact on the thermal properties of the films, although it simultaneously enhances the mechanical and interfacial properties of the material.

 Received 16th October 2025  
 Accepted 6th February 2026

DOI: 10.1039/d5ra07926h

[rsc.li/rsc-advances](https://rsc.li/rsc-advances)

## Introduction

Worldwide plastic consumption has increased since its introduction to the industrial world, making plastic essential across various industries, particularly in the packaging sector, which accounts for 40% of total plastic use in industrial production<sup>1</sup> around the world. The advantages of plastic materials include but are not limited to their low cost, light weight, and ease of manipulation. However, the sources and the inherent recyclability of most plastics are considered unsustainable.<sup>2,3</sup>

The growing demand for polymers is partially addressed by the production of biocompatible plastics as alternatives to non-renewable materials.<sup>4</sup> These plastics often meet market requirements while being highly biodegradable or compostable, which prevents environmental accumulation.<sup>5</sup> Similar to

conventional petroleum-based plastics, many bioplastics can be recycled, thus extending their lifecycle beyond single-use applications.

In this context, poly(lactic acid) (PLA) stands out as one of the most promising polymers among renewable and biodegradable options.<sup>6</sup> PLA is an aliphatic polyester that can be derived from renewable food waste sources, such as starch-containing materials.<sup>7</sup> However, the synthesis methods involving waste biomass are still under development. It is worth mentioning that PLA's production cost remains high, making it less competitive for use as a general-purpose polymer.<sup>8</sup> One solution to this issue is to blend PLA with other less expensive polymers or fillers, but a far more impactful criterion is to impart to the material advanced features so as to increase its inherent value.

Regulatory compliance issues continue to arise when using PLA in the food industry, with safety approvals primarily focused on material composition, processing methods, and the use of additives and solvents. Additionally, PLA's inherent thermal limitations restrict its application to cold food packaging only.<sup>9</sup>

In the biomedical field, PLA is commonly used for implants, scaffolding, and drug delivery systems due to its degradation into lactic acid, a monomer naturally metabolized by the human body. However, it still faces challenges, such as low mechanical strength, high hydrophilicity, and slow degradation rates, which can limit its effectiveness in certain applications.<sup>10,11</sup>

In this context, this paper aims to present a new method for casting bioplastic films to produce highly dense PLA composites. Such materials can potentially find their way to a vast range of applications, from the food packaging industry to the

<sup>a</sup>Department of Computer, Modeling, Electronics and Systems Engineering, University of Calabria, Via P. Bucci Cubo 42C, Rende, 87036, CS, Italy. E-mail: sudip.chakraborty@unical.it; stefano.curcio@unical.it

<sup>b</sup>Department of Mechanical, Energy, and Management Engineering, University of Calabria, Via P. Bucci Cubo 46C, Rende, 87036, CS, Italy

<sup>c</sup>Institute on Membrane Technology, National Research Council of Italy (ITM-CNR), Cubo 17C, Via Pietro Bucci, Rende 87036, Italy

<sup>d</sup>ENEA, Italian National Agency for New Technologies, Energy and Sustainable Economic Development, Trisaia Research Centre, S.S. 106 Ionica, km 419 + 500, 75026 Rotondella, MT, Italy

<sup>e</sup>Department of Biology, Ecology and Earth Sciences, Centre for Microscopy and Microanalysis (CM2), Transmission Electron Microscopy Laboratory, University of Calabria, Via P. Bucci, 87036 Arcavacata di Rende, CS, Italy

<sup>f</sup>Nanotec Institute-National Research Council (CNR-NANOTEC), Rende Secondary Unit, Via-P. Bucci, Cube 31/c, 87036-Rende, CS, Italy

<sup>g</sup>Institute of Bioprocess Engineering and Pharmaceutical Technology (IBPT), Technische Hochschule Mittelhessen (THM), Gutfleischstraße 3, 35390 Gießen, Germany



biomedical world (e.g.: controlled release, prosthetic coatings) by potentially overcoming the current limits of PLA. In this context, this work investigates how this method, together with varying plasticiser-to-PLA ratios, affects the physical properties of the resulting films.

PLA films produced through solvent casting are often utilised solvents with high affinity for PLA, such as chloroform, methylene chloride, and acetonitrile, which can be used at room temperature.<sup>12</sup> To explore a safer procedure, this study uses ethyl acetate, a food-safe ester solvent, as an alternative to the standard solvents, which are generally considered unsuitable for food and physiological use.<sup>13,14</sup>

The novel air-induced temperature-controlled phase separation (AITCPS) solvent casting technique is introduced in this study for the first time, as it offers advantages over traditional extrusion casting, specifically in producing films with desired denseness and thickness. The impact of the plasticiser on these properties is discussed in subsequent sections.

Regarding the mechanical properties, a common drawback of PLA is its inherent brittleness, which poses challenges for its broad use. Since polymer films must exhibit significant deformation capability, various fillers and plasticisers are commonly added to improve their properties.<sup>15</sup> In this study, glycerol (G) was selected as the plasticiser due to its high biocompatibility, low cost, and availability. Glycerol small molecular size and multiple hydroxyl groups enable strong hydrogen bonding with polar polymers such as PLA, reducing intermolecular interactions and increasing chain mobility. As a result, glycerol improves flexibility at relatively low concentrations. In addition, glycerol is food-grade, non-toxic, and generally recognized as safe (GRAS), making it suitable for food-contact applications. Its low volatility and good processability, combined with low cost and wide availability, further support its selection. Other plasticizers such as sorbitol and polyethylene glycol (PE) could be also suitable for the scope, but compared with glycerol, sorbitol has a higher molecular weight and lower mobility, which generally results in reduced plasticisation efficiency but improved resistance to migration. In addition, sorbitol often requires higher loadings or coplasticisers to achieve comparable flexibility in PLA. PEG offers tunable plasticisation depending on molecular weight, typically showing high miscibility with PLA, providing an effective balance between flexibility and stability. However, low-molecular-weight PEG may migrate, while higher-molecular-weight PEG is less efficient in plasticity enhancement. Overall, glycerol is ideal for its efficiency and safety, while sorbitol and PEG may be preferred when improved moisture resistance is required.

The casting method plays a crucial role in determining the final properties of the films. In this study, PLA solutions with different concentrations of G were prepared and cast using an automatic film casting machine employing the AITCPS technique. This approach guarantees precise control over film thickness and produces uniform G/PLA blends without defects, ensuring consistent morphological and mechanical properties across all samples.

## Experimental procedures and characterization

### Materials

Materials used for the sample preparation were PLA (3 mm nominal granule size, biopolymer, large molecular weight distribution centered at 230 000 g mol<sup>-1</sup>, melting point 172 °C, tradename Goodfellow 459-898-81, purchased via Merck KGaA, Darmstadt, Germany), ethyl acetate (EA) ACS, 99.5% (VWR Chemicals) used as solvent, and glycerol ACS reagent ≥99.5% (Sigma Aldrich) used as plasticiser.

### Sample casting

PLA granules, before their use, were desiccated at 120 °C for 24 hours in a ventilated oven (Binder ED32) to remove any residual water content.<sup>16</sup> PLA granules were then solubilised in ethyl acetate (EA). Initially, 3 g of PLA were added to 30 g of EA using a 250 mL three-neck round flask to obtain. All samples were prepared starting from. Different ratios of G were added to create different composites, resulting in a series of samples with a fixed PLA content and increasing G concentrations, as summarised in Table 1.

The flask was bathed in a shallow glass container filled with water in contact with a heating and stirring plate. Furthermore, the flask was equipped with a reflux condenser kept at 12 °C (Fig. 1) to prevent solvent loss. G was at this point added to the prepared batch under continuous stirring at 400 rpm. The system was then heated at 73 °C under continuous stirring and kept at the same temperature for 60 minutes to ensure complete PLA dissolution. Heating was provided in order to overcome the near insolubility of PLA in EA at room temperature.<sup>17</sup> Temperature monitoring was carried out using a thermocouple (TFA Lab Thermometer IP65) in contact with the solution through one of the secondary outputs of the flask (with the inlet sealed to prevent leakage). After preparation, the solution was cooled down to 45 °C while stirring.

Film casting was carried out using an automatic casting machine (Porometer Memcast). The prepared solutions were poured into the reservoir of the casting knife, set to a 500 μm gap.

The casting plate temperature was maintained at 35 °C, ensuring a temperature difference of 10 °C between the casting solution and the plate. This was done to avoid excessive

Table 1 PLA/G sample percentages

Sample	PLA/EA [wt/wt%]	G/PLA [wt/wt]
S00	10.0	0.00
S05	10.0	0.05
S10	10.0	0.10
S15	10.0	0.15
S20	10.0	0.20
S40	10.0	0.40
S50	10.0	0.50
S60	10.0	0.60
S70	10.0	0.70



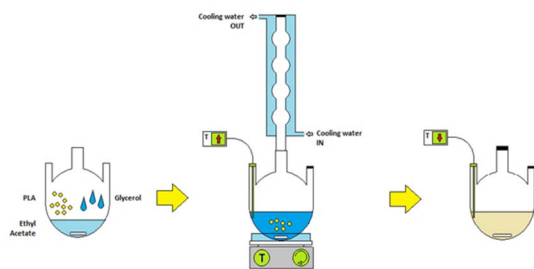


Fig. 1 Scheme of the sample preparation method.

temperature gradients that could lead to unwanted diffusive mass fluxes and stress in the film. The AITCPS casting velocity was set to  $1 \text{ cm s}^{-1}$ , slow enough to allow the viscous solution to relax internal extrusion stresses during casting.<sup>18,19</sup> The casting machine was operated under controlled solvent evaporation rates, which are crucial for forming a dense film layer. After casting, the film was submerged in distilled water to remove any residual solvent and then dried at ambient temperature overnight.<sup>20</sup>

### Sample characterization

Functional groups of the prepared films were evaluated by collecting infrared spectra of the membrane surface in Attenuated Total Reflection (ATR) mode using an FT-IR ATR Spectrometer (PerkinElmer, Spectrum One).

Water contact angles (WCA) on the top surface of the casted films were measured using the sessile drop method at ambient temperature with a CAM 200 contact angle meter (KSV Instruments Ltd, Helsinki, Finland). A drop of water was deposited on the membrane surface using an automatic micro syringe to form the sessile drop. At least six measurements have been taken at different random spots on the sample surface.

Thermal characterization of the samples was carried out using thermal gravimetric analysis (TGA) and differential scanning calorimetry (DSC). For TGA, approximately 10 mg of each sample was cut from the specimens, placed into an  $\text{Al}_2\text{O}_3$  crucible, and analysed using a TGA 209 F1 Libra (Netzsch). The samples were heated from room temperature to  $500 \text{ }^\circ\text{C}$  at a rate of  $10 \text{ }^\circ\text{C min}^{-1}$  under a nitrogen atmosphere ( $40 \text{ mL min}^{-1}$ ).<sup>21</sup>

For DSC analysis, samples weighing between 5 and 10 mg were cut from the specimens and placed in a sealed aluminium pan. The analysis was performed using a DSC 300 Caliris (Netzsch). The samples underwent a two-step thermal program: first, a heating step, followed by a cooling step, and then a second heating step. The parameters were set as follows: the starting temperature was  $0 \text{ }^\circ\text{C}$ , with the samples heated at  $10 \text{ }^\circ\text{C min}^{-1}$  to  $250 \text{ }^\circ\text{C}$  under a nitrogen atmosphere. After 2 minutes of stabilisation, the cooling rate was set to  $10 \text{ }^\circ\text{C min}^{-1}$  back to  $0 \text{ }^\circ\text{C}$ . The second heating stage, conducted under the same conditions as the first, was performed to examine the material's properties without any thermal history.<sup>22</sup> The glass transition temperature ( $T_g$ ), cold crystallisation temperature ( $T_{cc}$ ), and melting temperature ( $T_m$ ) were determined from the first and second heating scans. The crystallinity ( $X_c$ ) percentage was calculated using eqn (1).<sup>23</sup>

$$X_c \% = \frac{H_m}{H_m^{\text{id}}} \times 100 \quad (1)$$

In the proposed equation,  $\Delta H_m$  is the measured heat of fusion, and  $\Delta H_m^{\text{id}}$  is the melting enthalpy of 100% crystalline PLA, which is assumed to be  $93.6 \text{ (J g}^{-1}\text{)}$ .<sup>24</sup>

Mechanical tests were conducted to assess the tensile properties and tear resistance of the films. Tensile testing was performed according to ASTM D882-18 (ASTM International).<sup>25</sup> PLA sheets were cut into 9 mm-wide strips. The thickness of each sample was determined through scanning electron microscope (SEM) image analysis (Thermo Scientific Phenom Pure). Testing was carried out using an electromechanical testing machine, MTS Criterion Model 42 (MTS Corporation, USA), with a cross-head displacement rate set to  $12.5 \text{ mm min}^{-1}$ , as recommended for low-deformable films (*i.e.*, with elongation less than 20%). The initial grip separation was fixed at 10 mm. At least five tests were conducted on each sample.

The tensile tests provided the following mechanical properties: Young's modulus ( $E$ ), maximum strength ( $\sigma\text{-max}$ ), and elongation at break ( $\epsilon\text{-brk}$ ). Strain measurements were obtained using the Digital Image Correlation (DIC) technique. A high-resolution camera (GigE, Prosilica GT) with a resolution of  $2448 \times 2050$  pixels (pixel size:  $3.45 \text{ } \mu\text{m} \times 3.45 \text{ } \mu\text{m}$ ) was used to capture images of the samples during testing, through an acquisition board (DAQ-STD-8D, National Instruments) with an acquisition speed of 15 fps. Image analysis was performed using the VIC-2D software (Correlated Solutions).

Water vapour transmission rate (WVTR) tests were performed to evaluate the effect of increasing plasticiser content in the PLA matrix on water vapour permeation. This property is particularly important for food packaging applications, as the ability of the packaging to retain water vapour directly impacts the spoilage rate of the enclosed food.

The WVTR tests are based on a gravimetric procedure: samples were placed in a 100 mL aluminium cell with a sealed top. The top had a central opening with an area of  $10 \text{ cm}^2$ . The cell was filled with 80 mL of distilled water to create the necessary headspace for water vapour generation, while the sample was positioned under the top (Fig. 8a). The entire setup was maintained at  $30 \text{ }^\circ\text{C}$  with controlled external humidity set at 30%, and the cell weight was recorded every 30 minutes over 6 hours. Steady-state evaporation values were obtained throughout the evaporation period with minimal error.<sup>26</sup>

Since the focus of this study is the potential application of the obtained material in the food and medical industry, antimicrobial tests were also conducted at three different G ratios to evaluate the efficacy of the composites in inhibiting bacterial growth.<sup>27</sup> In this study, the effects of the produced films on *Staphylococcus aureus* (SA) – a Gram-positive bacterium responsible for acute infections. The antibacterial tests were conducted – on three different samples for each G ratio – in parallel, with each test including a control sample, where bacterial growth was measured on the film containing only PLA with no G. The tests were performed for each repetition on two initial inoculum dilutions:  $1 \times 10^{-2}$  CFU and  $1 \times 10^{-2}$  CFU.



## Results and discussion

Some of the resulting samples are shown in Fig. 2, where a decrease in transparency is evident in samples with higher G content, in particular for samples S05, S10, and S20.

The proposed method is suitable for scaling up to a continuous casting process, as illustrated in Fig. 3. The process consists of several stages: a solution tank, a break-up tank where the solution temperature is reduced to the pouring temperature, a pouring and rollers chamber with controlled solvent vapour concentration, a solvent recovery unit, and a final water bath for residual solvent removal.

### FT-IR analysis

FT-IR analyses were performed to confirm the presence of the plasticiser in the plasticised films. In Fig. 4 the obtained spectra for different prepared samples are shown.

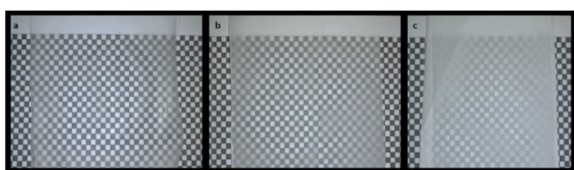


Fig. 2 Transparency of three of the PLA/G films prepared: S05 (a), S10 (b), S20 (c).

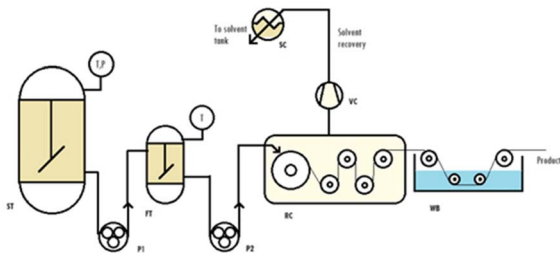


Fig. 3 Proposed scale up to a continuous casting process.

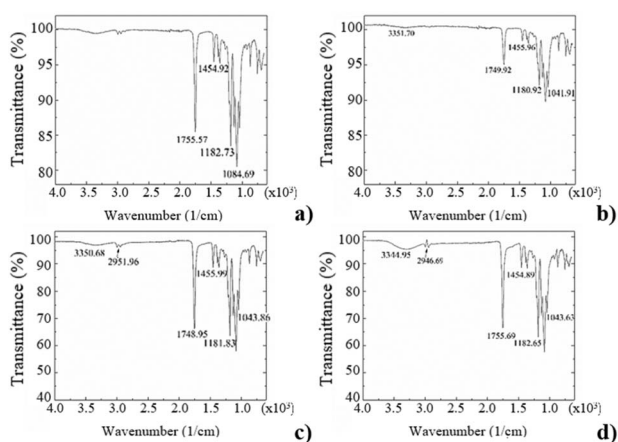


Fig. 4 FT-IR spectra of samples S10, S20, S70, S80 (a–d).

FT-IR analysis of the pristine PLA film reveals a peak at  $1755.57\text{ cm}^{-1}$ , corresponding to the stretching vibration of the C=O bond in the ester groups. Additionally, the band at  $1454.92\text{ cm}^{-1}$  is attributed to the deformation of C–H bonds in the methyl group.<sup>21</sup> Peaks at  $1180\text{ cm}^{-1}$  and  $1080\text{ cm}^{-1}$  are associated with C–O–C bond stretching.<sup>16</sup> These peaks were also observed in the plasticised samples. The presence of the plasticiser is indicated by a band around  $3500\text{ cm}^{-1}$ , which corresponds to the stretching vibration of O–H bonds, likely due to intermolecular or intramolecular hydrogen bonding. Furthermore, a less pronounced peak around  $3000\text{ cm}^{-1}$  is attributable to the –CH groups in the plasticiser.<sup>28</sup>

### Water contact angle (WCA)

The water contact angle (WCA) of the pure PLA film, which is reported in the literature to fall within the range of  $75^\circ$ – $85^\circ$ , was measured to be  $87.5^\circ \pm 1.8$ .<sup>29,30</sup> The addition of the plasticiser resulted in a reduction in the WCA as shown in Fig. 5, likely due to the introduction of hydrophilic surface groups that enhance the interaction between water and the film surface.

Contact angle values refer to stable angle values after an initial drop spreading, which was witnessed during an initial

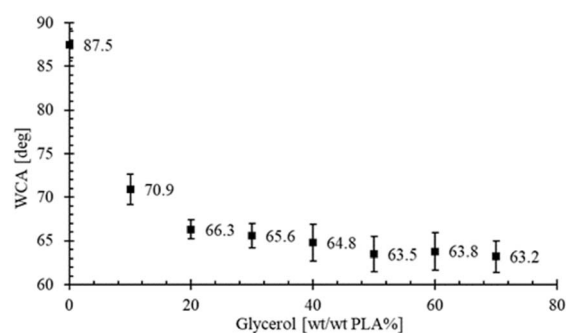


Fig. 5 WCA values of the PLA/G samples plotted against samples G content.

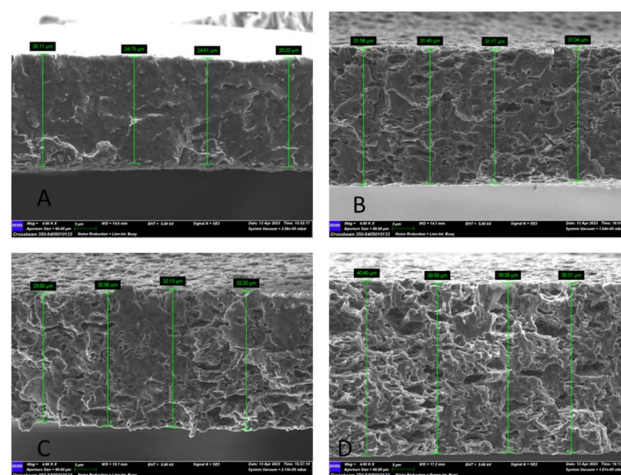


Fig. 6 SEM images (cross sections) of samples with thickness quotes at increasing plasticizer content. Figures (A) to (D) are respectively relative to samples S00, S20, S40 and S60.



time span of 60–80 seconds. As mentioned previously, the addition of the plasticiser led to a significant reduction in the water contact angle (WCA) due to the interaction of the –OH groups with water; this effect is more pronounced at lower plasticiser ratios: WCA values decrease as the plasticiser content increases, with an asymptotic trend observed at higher ratios. The WCA value stabilises at approximately 63° at the highest plasticiser ratio, following a monotonic trend throughout the entire range.

### Scanning electron microscopy (SEM)

SEM imaging was conducted using a ZEISS Cross Beam 350 (Fig. 6). Cross-sectional images of the samples reveal that the addition of higher plasticiser amounts significantly impacts the morphology, resulting in a less dense polymer matrix and an increase in sample thickness. As discussed in the following sections, this morphological change plays a crucial role in the other characterisations. SEM cross-sectional imaging clearly shows that higher plasticiser content leads to the formation of a polymer matrix with increased void ratios, particularly when

compared to the neat PLA sample, which appears much denser. Notably, the addition of plasticiser did not affect the casting procedure in terms of solvent evaporation rates or result in stratification, as no evidence of inner layers with different morphologies and void ratios was observed.<sup>31</sup>

### Thermal stability

Thermal gravimetric analysis (TGA) and differential scanning calorimetry (DSC) were conducted to investigate the effect of plasticiser addition on the crystallinity and thermal degradation behaviour of the polymer matrix. The results are presented in Fig. 7 and are discussed in the following section. For a better comparison, TGA and DSC were also performed on pure plasticiser and the pristine PLA granules.

TGA results reveal that the plasticiser degrades completely at temperatures below 250 °C. In Fig. 7a, TGA mass losses up to 250 °C are reported. TGA mass loss data at 250 °C for different samples (Fig. 7c) demonstrate a direct relationship between mass loss and plasticiser concentration (in weight fractions). A comparison with a 1 : 1 correlation indicates that, with minimal deviation, all mass loss occurring below 250 °C can be attributed to plasticiser degradation alone, confirming that the entire plasticiser content in the samples degrades under these conditions. Another notable effect is the stripping of water from the plasticiser at higher ratios, evident in samples with plasticiser ratios above 50%.

DSC results, shown in Fig. 7b, indicate that the presence of plasticiser did not affect the crystallisation ratio of the samples. Specifically, no significant changes were observed in the area under the main peak around 150 °C. The crystallinity of all samples remained close to 30 ± 5%.

More specifically, values for  $T_{cc}$ ,  $T_m$  and  $X_c$  resulting from the DSC tests are respectively  $107.4 \pm 1.2$  °C,  $150 \pm 2.5$  °C and  $44.9 \pm 3.8\%$  for all samples; while the inclusion of plasticiser resulted in a slight increase of  $T_g$  of approximately 8 °C (from 47.3 °C to  $65.0 \pm 2.6$  °C). This change appears independent of the plasticiser ratios, suggesting that the presence of G does not substantially affect the mobility of the polymer chains in the amorphous state or the melting temperature.

### Mechanical properties

The influence of plasticiser addition on the mechanical properties of PLA samples was investigated, and the main mechanical properties derived from the load–displacement curves are presented in Table 2. Samples fabricated with neat PLA exhibit

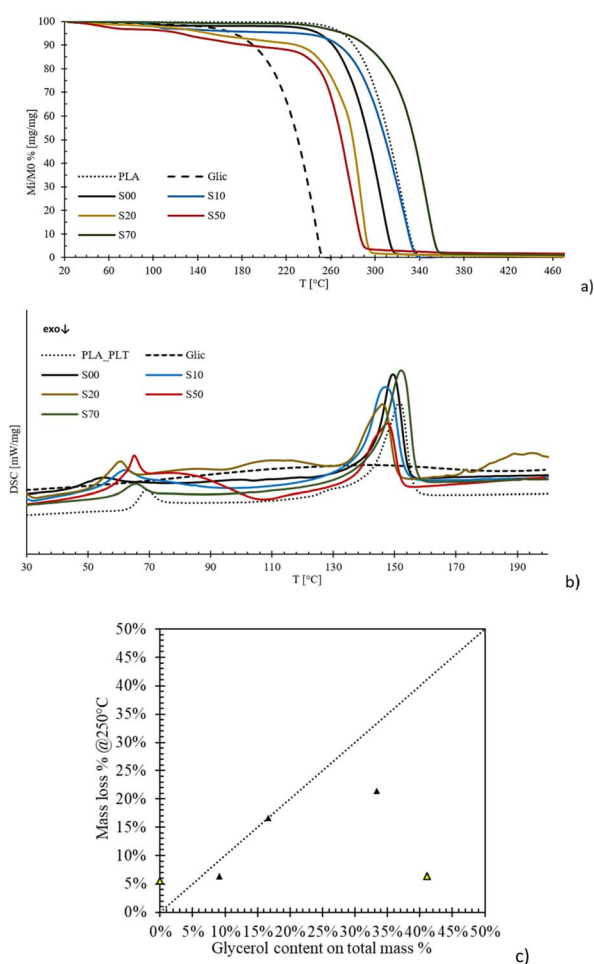


Fig. 7 TGA analysis results on PLA/G samples, pure plasticiser and PLA powder (a); DSC analysis results on PLA/G samples and PLA powder (b); total mass loss (TGA analysis) at 250 °C in comparison to G mass percentage used for sample preparation (c).

Table 2 Mechanical properties of PLA samples

Sample	$E$ [GPa]	$\sigma_{max}$ [MPa]	$\epsilon_{brk}$ [mm mm <sup>-1</sup> ]
S00	$2.97 \pm 0.20$	$52.48 \pm 7.14$	$0.022 \pm 0.005$
S10	$2.16 \pm 0.12$	$32.82 \pm 0.92$	$0.049 \pm 0.008$
S20	$1.80 \pm 0.05$	$28.32 \pm 0.99$	$0.052 \pm 0.011$
S30	$1.28 \pm 0.19$	$19.78 \pm 0.56$	$0.050 \pm 0.008$
S40	$1.28 \pm 0.10$	$17.57 \pm 0.41$	$0.035 \pm 0.013$
S50	$1.11 \pm 0.04$	$16.22 \pm 0.59$	$0.018 \pm 0.005$
S60	$0.87 \pm 0.07$	$11.34 \pm 1.18$	$0.016 \pm 0.007$



brittle behaviour, characterised by sudden failure, yet show good mechanical properties.

The mechanical properties of neat PLA samples are consistent with those reported in other studies (Sharma *et al.*, 2021).<sup>32</sup> Specifically, Sharma *et al.* (2021) reported the following values for tensile modulus, elongation at break, and maximum strength: 2.4 GPa, 5%, and 47 MPa, respectively. Any slight differences in the obtained results can be attributed to variations in the raw materials.

In terms of failure mechanisms, neat PLA samples exhibit brittle behaviour, characterised by sudden fracture and an abrupt load drop. The failure mechanisms of the plasticised samples remain similar to those of the neat PLA.

The addition of plasticiser consistently alters the mechanical properties of the PLA samples: it reduces the Young's modulus and maximum strength, while elongation at break is improved. The reduction in mechanical properties is strongly linked to the increased channelling and higher porosity observed at higher G ratios, resulting in a weaker matrix overall.<sup>33</sup> Samples with higher G content show an increased elongation at break, with an optimal peak observed for samples with intermediate G ratios—those that do not experience the aforementioned stripping effect. This result aligns with the expected plasticising effect, which generally improves ductility but tends to reduce other mechanical properties.<sup>34</sup> The best compromise between ductility and mechanical properties was achieved with low G ratio samples, while samples with intermediate plasticiser ratios exhibited the highest deformations and thus the best performance in terms of elongation.

### Water vapour transpiration rate (WVTR)

WVTR test results reported in Fig. 8 demonstrate that, up to a certain level, an increase in the plasticiser concentration leads to higher vapour transpiration.<sup>35</sup> The value for the control sample S00 aligns well with literature data, showing a value of  $1.73 \text{ mg} (\text{h cm}^2)^{-1}$ , compared to the  $1.52 \text{ mg} (\text{h cm}^2)^{-1}$  reported by Shogren.<sup>36</sup> Two distinct behaviours were observed: a steep increase at lower plasticiser concentrations and a slower increase at higher concentrations, resulting in a sigmoid-like, non-linear dependency across the entire concentration range. To accurately capture the WVTR profile in the region with the

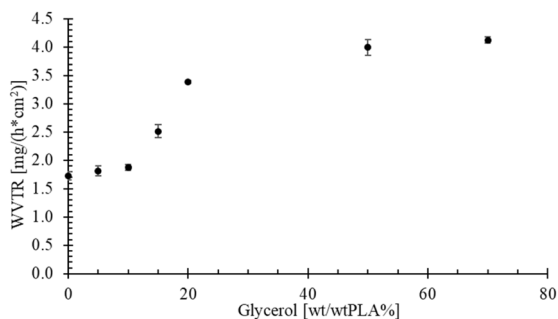


Fig. 8 WVTR results at 30 °C plotted against plasticizer percentages, a scheme of the test cell is reported in the low right angle of the graph.

steepest changes, samples with very low G ratios (0.05 and 0.15 wt/wt PLA) were included in the study. The observed trend corresponds with SEM observations, where higher G ratios lead to greater matrix void ratios and more extensive channelling, so that the increased channelling creates easier pathways for water vapour to permeate through the film. This effect is clearly tunable through the casting methodology and plasticiser content.

### Antimicrobial activity

To evaluate the antibacterial properties of the samples, a quantitative test using Gram-positive bacteria *Staphylococcus aureus* (SA) was conducted. Some of the microbial counting plates, tested at  $10^{-2}$  CFU are shown in Fig. 9. Results of the antimicrobial tests showed that for the control sample, the culture counts were approximately  $6.8 \times 10^3 \pm 2.2 \times 10^3 \text{ CFU cm}^{-2}$ .

The films containing different G concentrations (5, 10 and 20% wt) showed significant bacterial growth inhibition (see Table 3). Higher cell growth reduction ( $\approx 99\%$ ) was obtained with a G ratio of 20%wt. Therefore, the addition of the plasticiser, provides excellent antibacterial properties against the SA strains, in accordance with previous literature data.<sup>37</sup>

Antimicrobial tests results are reported in Table 3. Results here are expressed in terms of logarithmic CFU reduction in respect to S00 samples, for each of the samples analysed and for the two inoculum dilutions tested.

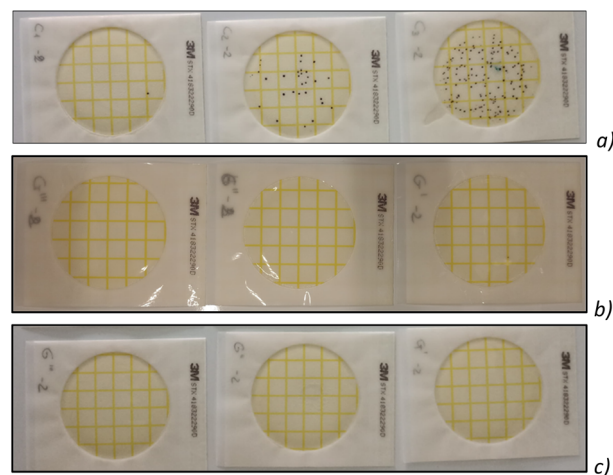


Fig. 9 Microbial count plates for control sample S00 (a), sample S10 (b) and sample S20 (c).

Table 3 *Staphylococcus aureus* antimicrobial test results

Sample	$10^{-2}$ CFU	$10^{-3}$ CFU
S20	99%	93%
S10	95%	90%
S05	92%	78%



## Conclusions

PLA is a valuable polymer for both food packaging and biomedical applications. To meet food safety standards, PLA films were cast using a more food-safe green solvent, as opposed to the commonly used standardised solvents for PLA. A novel casting method, Air Induced Temperature Controlled Phase Separation (AITCPS), resulted in a plasticised dense PLA composite with highly tunable properties.

Plasticisers are essential for achieving the desired mechanical properties in polymer films. In this study, glycerol proved to be an effective alternative to more traditional additives, particularly due to its high compatibility with food and physiological environments. A key feature of the study is the interaction between glycerol and PLA during the casting process: varying fractions of plasticiser lead to significantly different results, particularly in terms of film morphology. Higher glycerol concentrations result in highly porous films, which critically affect the mechanical properties, leading to lower yields and higher elongation at break.

The effect of the plasticiser ratio on the thermal properties of the films was minimal, while its influence on the mechanical and interfacial properties was dramatic. Specifically, WCA values decreased as the glycerol ratio increased, exhibiting an asymptotic trend at higher ratios, which imparted a more hydrophilic character to the material.

WVTR tests showed that increasing glycerol concentrations raised transpiration, with a steep change observed around 10–20% wt ratios of G. This resulted in a sigmoid-like relationship across the entire range of concentrations.

Mechanical testing confirmed the expected plasticising effect: improved ductility (elongation at break) together with a decrease in elastic modulus and yield stress. The best balance between ductility and other mechanical properties was achieved with low glycerol ratio samples, while samples with intermediate plasticiser ratios performed best in terms of deformation.

Antimicrobial tests show how even minimal amounts of G have a huge impact on the activeness of the material, this result being very critical in sight of a profitable use of the composite as active food packaging, prosthetic coating or controlled release medium. Further developments of this study should cover antimicrobial tests performed against multiple microbial strains, to be chosen between those relevant for food packaging and biomedical applications.

Still, to access the effective employment of the material, a strict assessment of the activation of the inflammatory response for biomedical applications should be tackled, together with the development of active mechanisms – inherent in the material itself – to control it.

Another aspect worth investigating soon is the modelling of the binary interactions between the material and the inflammatory response actors, as well as the fine modelling of material decay in the application environment, to acquire predictive abilities which allow further optimisation of the material and of the casting method.

In conclusion, the AITCPS methodology demonstrates strong potential, offering excellent opportunities for product optimisation and the tunability of key material features.

## Author contributions

Gerardo Coppola: writing – original draft, methodology, investigation, data curation; Sebastiano Candamano: data curation, and editing; Catia Algeri: conceptualisation, writing – review & editing; Corradino Sposato: investigation, data curation & editing; Chiara Morano: data curation, editing; Leonardo Pagnotta: review & editing; Mariano Davoli: data curation, material characterization and SEM analysis; Stefano Curcio: writing – review, editing, fund acquisition, resources; Sudip Chakraborty: conceptualisation, methodology, draft writing, review & final editing.

## Conflicts of interest

There are no conflicts to declare.

## Data availability

The data that support the findings of this study are available from the corresponding author(s), upon request.

## Acknowledgements

The authors thank @STAR, CNR-NANOTEC and MaTeRiA laboratories, “Progetto STAR 2-PIR01-00008”-Ministry of University and Research, for providing the equipment employed for experimental analysis.

## References

- 1 H. Oliver-Ortega, J. Tresserras, F. Julian, M. Alcalà, A. Bala, F. X. Espinach and J. A. Méndez, Nanocomposites Materials of PLA Reinforced with Nanoclays Using a Masterbatch Technology: A Study of the Mechanical Performance and Its Sustainability, *Polymers*, 2021, **13**, 2133, DOI: [10.3390/polym13132133](https://doi.org/10.3390/polym13132133).
- 2 A. Caliskan, N. Abdullah, N. Ishak, D. S. Ametefe and I. T. Caliskan, Systematic Literature Review on the Utilization of Tuber Crop Skins in the Context of Circular Agriculture, *Int. J. Recycl. Org. Waste Agric.*, 2024, **14**(1), 1–17, DOI: [10.57647/ijrowa-m1j8-w486](https://doi.org/10.57647/ijrowa-m1j8-w486).
- 3 M. A. Elsayy, K.-H. Kim, J.-W. Park and A. Deep, Hydrolytic Degradation of Polylactic Acid (PLA) and Its Composites, *Renew. Sustain. Energy Rev.*, 2017, **79**, 1346–1352, DOI: [10.1016/j.rser.2017.05.143](https://doi.org/10.1016/j.rser.2017.05.143).
- 4 G. Coppola, M. T. Gaudio, C. G. Lopresto, V. Calabro, S. Curcio and S. Chakraborty, Bioplastic from Renewable Biomass: A Facile Solution for a Greener Environment, *Earth Syst. Environ.*, 2021, **5**, 231–251, DOI: [10.1007/s41748-021-00208-7](https://doi.org/10.1007/s41748-021-00208-7).
- 5 G. Kale, T. Kijchavengkul, R. Auras, M. Rubino, S. E. Selke and S. P. Singh, Compostability of Bioplastic Packaging



- Materials: An Overview, *Macromol. Biosci.*, 2007, 7, 255–277, DOI: [10.1002/mabi.200600168](https://doi.org/10.1002/mabi.200600168).
- 6 J. Pretula, S. Slomkowski and S. Penczek, Polyactides—Methods of Synthesis and Characterization, *Adv. Drug Delivery Rev.*, 2016, 107, 3–16, DOI: [10.1016/j.addr.2016.05.002](https://doi.org/10.1016/j.addr.2016.05.002).
- 7 M. Singhvi and D. Gokhale, Biomass to Biodegradable Polymer (PLA), *RSC Adv.*, 2013, 3, 13558, DOI: [10.1039/c3ra41592a](https://doi.org/10.1039/c3ra41592a).
- 8 I. Spiridon, K. Leluk, A. M. Resmerita and R. N. Darie, Evaluation of PLA–Lignin Bioplastics Properties before and after Accelerated Weathering, *Composites, Part B*, 2015, 69, 342–349, DOI: [10.1016/j.compositesb.2014.10.006](https://doi.org/10.1016/j.compositesb.2014.10.006).
- 9 J. O'Loughlin, D. Doherty, B. Herward, C. McGleenan, M. Mahmud, P. Bhagabati, A. N. Boland, B. Freeland, K. D. Rochfort, S. M. Kelleher, *et al.*, The Potential of Bio-Based Poly(lactic acid) (PLA) as an Alternative in Reusable Food Containers: A Review, *Sustainability*, 2023, 15(21), 15312, DOI: [10.3390/su152115312](https://doi.org/10.3390/su152115312).
- 10 S. Shiva, R. G. Asuwin Prabu, G. Bajaj, A. E. John, S. Chandran, V. V. Kumar and S. Ramakrishna, A review on the recent applications of synthetic biopolymers in 3D printing for biomedical applications, *J. Mater. Sci.: Mater. Med.*, 2023, 34(12), 62, DOI: [10.1007/s10856-023-06765-9](https://doi.org/10.1007/s10856-023-06765-9).
- 11 L. Ranakoti, B. Gangil, P. Bhandari, T. Singh, S. Sharma, J. Singh and S. Singh, Promising Role of Poly(lactic acid) as an Ingenious Biomaterial in Scaffolds, Drug Delivery, Tissue Engineering, and Medical Implants: Research Developments, and Prospective Applications, *Molecules*, 2023, 28(2), 485, DOI: [10.3390/molecules28020485](https://doi.org/10.3390/molecules28020485).
- 12 T. Angelin Swetha, A. Bora, K. Mohanrasu, P. Balaji, R. Raja, K. Ponnuchamy, G. Muthusamy and A. Arun, A comprehensive review on poly(lactic acid) (PLA) – Synthesis, processing and application in food packaging, *Int. J. Biol. Macromol.*, 2023, 234, 123715, DOI: [10.1016/j.ijbiomac.2023.123715](https://doi.org/10.1016/j.ijbiomac.2023.123715).
- 13 D. J. Marino, Ethyl Acetate, in *Encyclopedia of Toxicology*, Elsevier, 2005, pp. 277–279 ISBN 978-0-12-369400-3.
- 14 K. Duarte, C. I. L. Justino, A. M. Gomes, T. Rocha-Santos and A. C. Duarte, Chapter 4 - Green Analytical Methodologies for Preparation of Extracts and Analysis of Bioactive Compounds, *Comprehensive Analytical Chemistry*, Elsevier, 2014, vol. 65, pp. 59–78,.
- 15 N. Petchwattana, J. Sanetuntikul and B. Narupai, Plasticization of Biodegradable Poly(Lactic Acid) by Different Triglyceride Molecular Sizes: A Comparative Study with Glycerol, *J. Polym. Environ.*, 2018, 26, 1160–1168, DOI: [10.1007/s10924-017-1012-7](https://doi.org/10.1007/s10924-017-1012-7).
- 16 A. Iulianelli, C. Algieri, L. Donato, A. Garofalo, F. Galiano, G. Bagnato, A. Basile and A. Figoli, New PEEK-WC and PLA Membranes for H<sub>2</sub> Separation, *Int. J. Hydrogen Energy*, 2017, 42, 22138–22148, DOI: [10.1016/j.ijhydene.2017.04.060](https://doi.org/10.1016/j.ijhydene.2017.04.060).
- 17 U. Siemann, The solubility parameter of poly(DL-lactic acid), *Eur. Polym. J.*, 1992, 28(3), 293–297, DOI: [10.1016/0014-3057\(92\)90192-5](https://doi.org/10.1016/0014-3057(92)90192-5).
- 18 C. Kahrs, T. Gühlstorf and J. Schwellenbach, Influences of Different Preparation Variables on Polymeric Membrane Formation via Nonsolvent Induced Phase Separation, *J. Appl. Polym. Sci.*, 2020, 137, 48852, DOI: [10.1002/app.48852](https://doi.org/10.1002/app.48852).
- 19 E. Lasseguette, L. Fielder-Dunton, Q. Jian and M.-C. Ferrari, The Effect of Solution Casting Temperature and Ultrasound Treatment on PEBAX MH-1657/ZIF-8 Mixed Matrix Membranes Morphology and Performance, *Membranes*, 2022, 12, 584, DOI: [10.3390/membranes12060584](https://doi.org/10.3390/membranes12060584).
- 20 C. Algieri, S. Chakraborty and U. Pal, Efficacy of Phase Inversion Technique for Polymeric Membrane Fabrication, *J. Phase Change Mater.*, 2021, 1(1), DOI: [10.6084/jpcm.v1i1.10](https://doi.org/10.6084/jpcm.v1i1.10).
- 21 Z. Yang, X. Li, J. Si, Z. Cui and K. Peng, Morphological, mechanical and thermal properties of poly (lactic acid) (PLA)/cellulose nanofibrils (CNF) composites nanofiber for tissue engineering, *J. Wuhan Univ. Technol., Mater. Sci. Ed.*, 2019, 34(1), 207–215, DOI: [10.1007/s11595-019-2037-7](https://doi.org/10.1007/s11595-019-2037-7).
- 22 N. M. Nurazzi, N. Abdullah, M. N. F. Norrahim, S. H. Kamarudin, S. Ahmad, S. S. Shazleen, M. Rayung, M. R. M. Asyraf, R. A. Ilyas and M. Kuzmin, Thermogravimetric Analysis (TGA) and Differential Scanning Calorimetry (DSC) of PLA/Cellulose Composites, in *Poly(lactic acid)-Based Nanocellulose and Cellulose Composites*, CRC Press, Boca Raton, FL, USA, 2022, pp. 145–164, ISBN 9781003160458.
- 23 W. H. Wan Ishak, N. A. Rosli and I. Ahmad, Influence of amorphous cellulose on mechanical, thermal, and hydrolytic degradation of poly(lactic acid)biocomposites, *Sci. Rep.*, 2020, 10, 11342, DOI: [10.1038/s41598-020-68274-x](https://doi.org/10.1038/s41598-020-68274-x).
- 24 E. W. Fischer, H. J. Sterzel and G. K. Z. Z. Wegner, Investigation of the structure of solution grown crystals of lactide copolymers by means of chemical reactions, *Kolloid-Z. Z. Polym.*, 1973, 251, 980–990.
- 25 ASTM D882, *Test Method for Tensile Properties of Thin Plastic Sheeting*, ASTM International, 2018.
- 26 B. Ganbarzadeh, A. Oromiehie, M. Musavi, K. Rezayi, E. Razmi and M. Jafar, Investigation of water vapour permeability, hydrophobicity and morphology of zein films plastized by polyols, *Iran. Polym. J.*, 2006, 15, 691–700.
- 27 ISO 22196:2011, Measurement of antibacterial activity on plastics and other non-porous surfaces, <https://www.iso.org/standard/54431.html>.
- 28 A. Krishnamurthy and P. Amritkumar, Synthesis and characterization of eco-friendly bioplastic from low-cost plant resources, *SN Appl. Sci.*, 2019, 1, 1432, DOI: [10.1007/s42452-019-1460-x](https://doi.org/10.1007/s42452-019-1460-x).
- 29 W. Wang, Y. Gong, Q. Sun, L. Li, A. Xu and R. Liu, High Performance Poly(vinyl Alcohol)/Poly(lactic acid) Materials: Facile Preparation and Improved Properties, *J. Appl. Polym. Sci.*, 2022, 139(26), 1–8, DOI: [10.1002/app.52470](https://doi.org/10.1002/app.52470).
- 30 B. D. Ratner, Surface Modification of Polymers: Chemical, Biological and Surface Analytical Challenges, *Biosens. Bioelectron.*, 1995, 10, 797–804, DOI: [10.1016/0956-5663\(95\)99218-A](https://doi.org/10.1016/0956-5663(95)99218-A).
- 31 Z. Kulinski and E. Piorkowska, Crystallization, structure and properties of plasticized poly(L-lactide), *Polymer*, 2005, 46(Issue 23), 10290–10300.



- 32 S. Sharma, A. Majumdar and B. S. Butola, Tailoring the biodegradability of polylactic acid (PLA) based films and ramie- PLA green composites by using selective additives, *Int. J. Biol. Macromol.*, 2021, **181**, 1092–1103, DOI: [10.1016/j.ijbiomac.2021.04.108](https://doi.org/10.1016/j.ijbiomac.2021.04.108).
- 33 N. Ljungberg and B. Wesslen, The effects of plasticizers on the dynamic mechanical and thermal properties of poly (lactic acid), *J. Appl. Polym. Sci.*, 2002, **86**(5), 1227–1234, DOI: [10.1002/app.11077](https://doi.org/10.1002/app.11077).
- 34 G. Ozkoc and S. Kemalogu, Morphology, biodegradability, mechanical, and thermal properties of nanocomposite films based on PLA and plasticized PLA, *J. Appl. Polym. Sci.*, 2009, **114**(4), 2481–2487, DOI: [10.1002/app.30772](https://doi.org/10.1002/app.30772).
- 35 P. Cazón, E. Morales-Sanchez, G. Velazquez and M. Vázquez, «Measurement of the Water Vapor Permeability of Chitosan Films: A Laboratory Experiment on Food Packaging Materials.» This, *J. Chem. Educ.*, 2022, **99**, 2403–2408.
- 36 R. Shogren, Water vapor permeability of biodegradable polymers, *J. Environ. Polym. Degrad.*, 1997, **5**, 91–95.
- 37 V. S. Saegeman, N. L. Ectors, D. Lismont, B. Verduyck and J. Verhaegen, Short- and long-term bacterial inhibiting effect of high concentrations of glycerol used in the preservation of skin allografts, *Burns*, 2008, **34**(2), 205–211, DOI: [10.1016/j.burns.2007.02.009](https://doi.org/10.1016/j.burns.2007.02.009).

